

# **2D LED Ising Model Simulation Using Monte Carlo Methods**

Cameron Jeffery and Fraser Lee

McGill University Department of Physics

Supervisor: Dominic Ryan

April 10, 2025

## Abstract

This experiment investigates the behaviour of a two-dimensional Ising model by way of an  $8 \times 8$  LED matrix as a physical analogue. By implementing a Metropolis-Hastings-based Monte Carlo simulation within an Arduino micro-controller, the LED matrix simulated the temperature dependent phase transitions between ordered and disordered magnetic states for three disjoint temperature regimes: Hot, Cold, and at the critical (Curie) temperature. The simulation permitted a real-time visualization of domain formation, while quantitative measurements of the energy, magnetisation, specific heat, and magnetic susceptibility were taken to reveal the thermodynamic trends across the three temperature regimes. The results of the experiment revealed high fidelity to the postulated behaviour of the Ising model that acts as a magnetic domain. In particular, the orientation of the spin states across the three temperature regimes coincided with hypothesized physical behaviour. Moreover, our observations align well with expected trends in each thermodynamic quantity.

## Contents

<b>1</b>	<b>Introduction</b>	<b>1</b>
1.1	Monte Carlo Simulation . . . . .	3
<b>2</b>	<b>Experimental Methods</b>	<b>4</b>
<b>3</b>	<b>Results</b>	<b>6</b>
<b>4</b>	<b>Discussion</b>	<b>10</b>
<b>5</b>	<b>Conclusion</b>	<b>11</b>

# 1 Introduction

This experiment examines a fundamental statistical mechanistic model for understanding ferromagnetic solids: the Ising Model. Coined by Wilhelm Lenz after his doctoral student Ernst Ising [1], the Ising Model gives a description of ferromagnetism, a phenomenon that arises when a collection of atomic spins align such that their associated magnetic moments point along the same axis, yielding a net macroscopic magnetic moment. In this experiment, we implement a physical analogue of a conceptual 2-dimensional Ising model, by way of an  $8 \times 8$  Adafruit LED matrix standing as an experimental proxy for the magnetic domain lattice. In the matrix, each LED represents a single atom's spin that can align up (denoted when the LED lights up), or down (when the LED is off). The system is held in equilibrium with a simulated thermal reservoir, the temperature of which is externally set by a photo-resistor or potentiometer. Snapshots of the spin-states of the lattice can be taken at any time by an Arduino Uno, acting as a “camera” into the simulation. We explore the model’s behaviour and dynamics across three different regimes: ordered (low temperature), critical, and disordered (high temperature).

In the Ising Model, these three macroscopic regimes arise entirely as a result of interactions between each dipole, and the neighbours orthogonally adjacent to it. Supposing that all atoms are identical spin- $1/2$  systems, it follows that for all  $i$ ,  $s_i = \pm 1$ , where  $s_i$  is the  $z$ -component of the  $i^{\text{th}}$  atomic spin. We characterise the total energy of the system as:

$$E = -J \sum_{i,j} s_i s_j. \quad (1)$$

Where  $J$  is the interaction term between the magnetic dipoles [2], set to unity for simplicity of this experiment. From Eq. 1, it is implied that spins that agree (lie parallel) will reduce the energy of the configuration, whereas spins that disagree (lie antiparallel) increase the energy.

We can furthermore characterise the Ising model as a statistical spin distribution given by  $\pi(s_i) \sim e^{E/kT}$ , prescribed by the partition function [3], where  $k$  is the Boltzmann constant,

and  $T$  is the temperature. From this, it can be concluded that at low temperatures, the system “freezes” around low-energy configurations. In other words, the system coheres with strong ferromagnetic alignment; in which the spins largely orient in the same direction. In our physical instantiation of the system, this experimentally looks like the LED matrix remaining largely homogeneous (that is, a predominant majority of the LEDs are either switched on, or off) when the temperature set-point of the thermal reservoir is low. To contrast, at high temperatures, the thermal energy overwhelms the structure of the system. The system becomes disordered and - in high temperature limit - all random spin configurations are equally likely. Lastly, for any ferromagnet, there exists a particular critical temperature, known as the phase-transition temperature or Curie temperature, where the expectation of the modulus of magnetisation  $\langle |M| \rangle$  becomes zero [4]. Physical chemist Lars Onsager derived the analytical solution to the critical temperature for a 2D Ising model as:

$$T_c = \frac{2J}{k \ln(1 + \sqrt{2})} \approx 2.27 \frac{J}{k} = 2.27T_0, \quad (2)$$

where  $T_0 \equiv \frac{J}{k_b}$  [5]. Furthermore, several observables can be investigated in this experimental setup. For instance, a quantitative measure of the magnetisation,  $M$ , which is defined as the average value of the spin:

$$|M| = \frac{1}{L^2} \left| \sum_{i=1}^N s_i \right|, \quad (3)$$

where  $L$  is the dimension of the 2D lattice, in this case, it is presumed that  $L = 8$  as given by the dimensions of the LED matrix. Since flipping of all spins simultaneously does not change the system energy, the modulus of the magnetisation is considered in this experiment. Similarly, the magnetic susceptibility,  $\chi$  is related to the fluctuations of the magnetisation by:

$$\chi = \frac{1}{k_b T} [\langle M^2 \rangle - \langle M \rangle^2]. \quad (4)$$

And finally, the specific heat of the system grants insight into how much the energy of the spin system changes with a varying temperature, and is defined as:

$$C_v = \frac{1}{T^2} [\langle E^2 \rangle - \langle E \rangle^2]. \quad (5)$$

## 1.1 Monte Carlo Simulation

In order to create a physical Ising Model system within the lab, we run a Metropolis-Hastings based Monte Carlo simulation, implemented on the Arduino UNO, to evolve the LED matrix of “spin configurations” in real time. This approach is stochastic, probabilistically accepting or rejecting spin flips based on the system’s partition function at a given temperature  $T$ . The key steps in the algorithm are:

- 1.** Spin Flip Proposal: A random spin  $s_i$  is selected from the  $8 \times 8$  LED lattice, with its current state (either  $+1$  or  $-1$ ) being flipped tentatively, or rather  $s_{i,j} \rightarrow s'_{i,j} = -s_{i,j}$ . Thus, a new state space of spins is obtained  $\mathcal{S} = \{s_{1,1}, \dots, s_{i,j}, \dots, s_{L,L}\} \rightarrow \mathcal{S}' = \{s_{1,1}, \dots, -s_{i,j}, \dots, s_{L,L}\}$ . From there, the resulting change in energy is calculated as  $\delta E = E(\mathcal{S}') - E(\mathcal{S})$ .
- 2.** Acceptance Probability: The proposed spin flip in the new state space,  $\mathcal{S}'$  is accepted as the new configuration with probability:

$$\mathbb{P}(s_{i,j} \rightarrow s'_{i,j}) = \begin{cases} 1 & \text{if } \delta E < 0 \\ \exp(-\delta E/kT) & \text{otherwise} \end{cases} \quad (6)$$

When  $\mathcal{S}'$  is rejected, we revert the system to  $\mathcal{S}$  [6].

- 3.** Repeat: One full “update” of the system corresponds to repeating the two previous steps  $L^2$  times. After these repartitions, the new configuration is drawn to the LED matrix, and taken as the system’s new state in the Monte Carlo simulation: the starting point from which to calculate the next update.

In addition, the LED matrix is assumed to have periodic boundary conditions; that is, the edge-cells interact with those on the opposite side. Topologically, this is equivalent to the embedding 2D lattice on the surface of a torus, and allows our simulated cell to approximate the dynamics a much larger system [7].

## 2 Experimental Methods

The experimental setup consisted of an Arduino UNO micro-controller paired with an Adafruit 8 × 8 LED matrix as the physically realized Ising lattice. Each LED represents a single spin: a lit LED representing a spin up dipole, and an unlit LED for spin down.

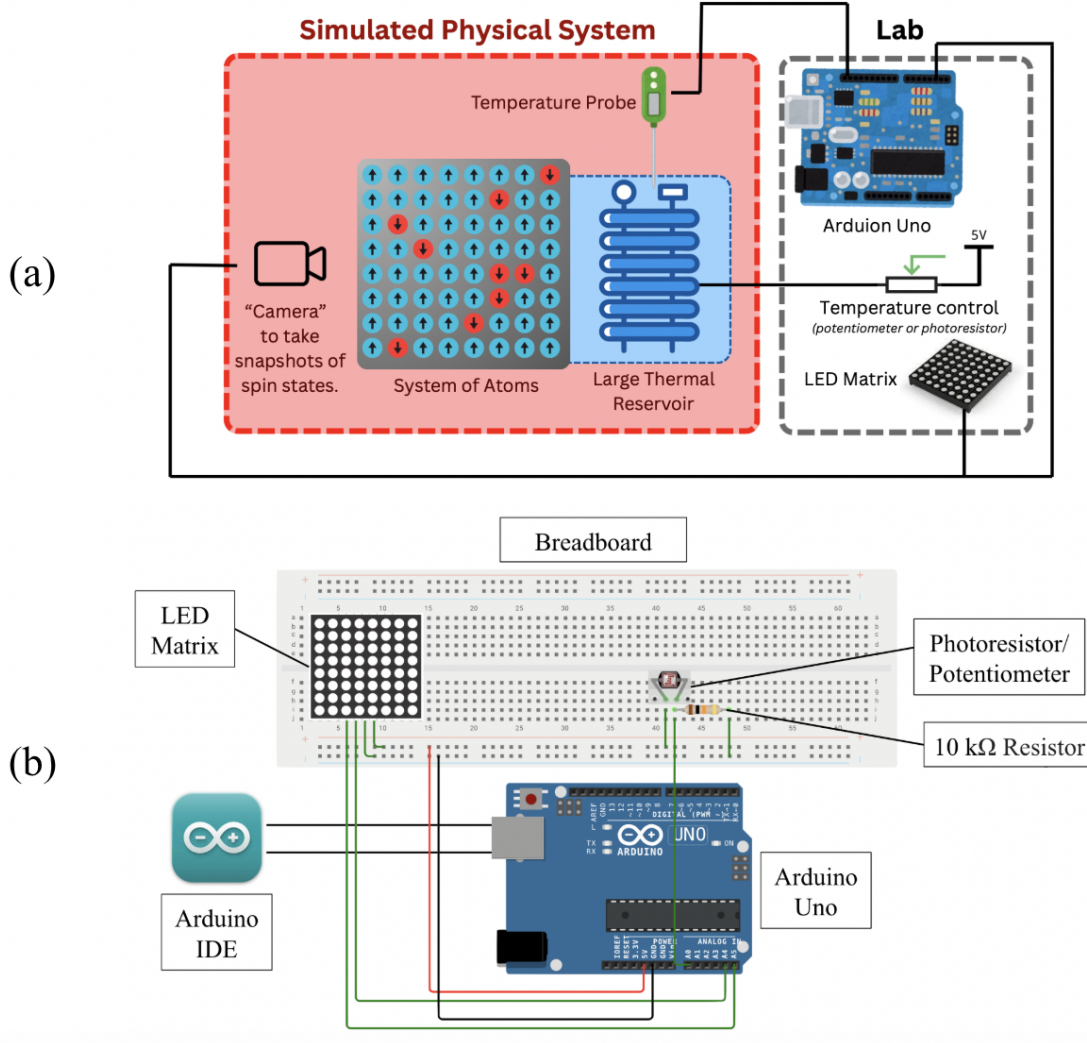


Figure 1: (a) Conceptual model of the experimental setup (b) Physical schematic of the experimental setup.

The temperature control was achieved through a photoresistor configured as a voltage divider with a  $10\text{ k}\Omega$  fixed resistor. The photoresistor's resistance varied with light intensity, producing an analog voltage read by the Arduino and mapped to a dimensionless temperature

parameter  $T$ . For measurements that demanded a continuous sweep of input temperature values, the setup opted for a potentiometer. The light intensity was varied to achieve the different temperature regimes for the Ising model. A schematic of the experimental setup is shown above in Fig. 1.

In the Arduino program, the raw analogue sensor value from the photoresistor,  $V_{\text{sensor}}$ , is and is subsequently scaled to produce a usable temperature range. This is achieved by obtaining a minimum analogue voltage value,  $V_{\min}$  (corresponding to the darkest condition), and a maximum analogue voltage value,  $V_{\max}$  (corresponding to the brightest condition), and thus the temperature of the thermal reservoir can be calculate via:

$$T = T_{\max} \cdot \left( \frac{V_{\text{sensor}} - V_{\min}}{V_{\max} - V_{\min}} \right) \quad (7)$$

Which is then used in our acceptance criterion described by Eq. 6. In this way, the photoresistor's voltage divider does not measure the absolute temperature, but instead provides a proportional control signal as to achieve simulations in the three broad temperature regimes discussed in Sec. 1. Then, the Monte Carlo routine was run; first for 1000 steps in the routine to allow the system to equilibrate at the given temperature setting, then for an additional 5000 steps for data collection

For all the thermodynamic observables we measured (presented in Figures 3, 4, 5, and 6), uncertainties were quantified by statistical binning. This approach was essential, since successive configurations of the LED matrix generated by the Metropolis algorithm are inherently correlated - a definitional consequence of the Markov chain process where each state is dependent on the previous one. During the production phase of the simulation, the 1000 steps Monte Carlo process was divided into 10 statistically independent bins, each of which contained 10 steps in the routine. Within each bin, the variance across each bin was measured and cited as the statistical error for each observable. This procedure was repeated independently for each temperature.

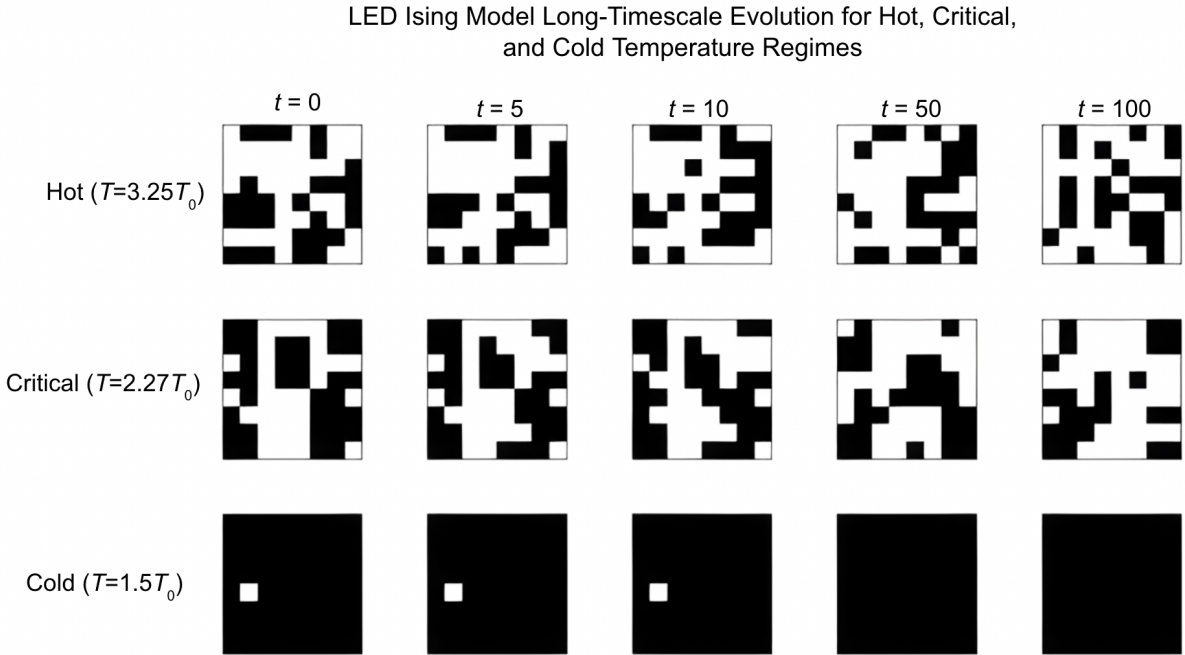


Figure 2: LED matrix states for hot, cold, and critical temperature regimes. The white cells indicate a LED light is turned on, and the black cells indicates the LED is turned off. Here,  $T_0 = J/k$ , where  $k$  is the Boltzmann constant, and  $J$  is the interaction term, which is set to unity.

### 3 Results

The dynamical evolution of the LED Ising system was captured through a series of snapshots at five key timesteps ( $t = 0, 5, 10, 50, 100$ ) for each of the three temperature regimes: cold ( $T = 1.5T_0$ ), hot ( $T = 20T_0$ ), and near the critical, or Curie temperature ( $T = T_C = 2.27T_0$ ).

The snapshots begin in the point of the simulation where the temperature equilibrates. That is, at  $t = 0$ , 1000 steps of the Monte Carlo simulation have passed. At steps thereafter, the timed snapshots were taken, with each instantaneous state representing the LED configuration immediately after completing the  $t$  – th Monte Carlo step. Recall each step consist of 64 spin flip attempts (equal to the number of LED lights). This is shown in Fig 2.

The thermodynamic behaviour of the 2D LED matrix Ising model is explored through key observables discussed in Sec. 1, namely, the magnitude of magnetisation, the energy, specific heat, and magnetic susceptibility, as plotted as a function of temperature. Sweeping through a range of temperature values with the potentiometer, appropriate data points were collect

using the following two-step procedure:

1. Equilibration: 1000 steps of the Monte Carlo simulation were required for the temperature to reach a steady-state. This is needed to ensure the initial configuration was “forgotten” to a sufficient degree for subsequent measurements.
2. Production phase: An additional 1000 steps were simulated, during which the observables were measured and binned. The measurement phase was divided into 10 bins of 100 steps each to appropriately consider uncertainties.

From there, appropriate data manipulation was required to adhere to the proper definitions of the observables as outlined in Sec. 1. These are calculated from the spin-state of the grid, measured through the “camera” described in Sec. 2. For instance, the energy of the LED system, as prescribed by Eq. 1, is the summed products of the neighbouring LED values (+1 for bright LED, -1 for a dark LED), and the magnetisation is the averaged absolute LED states across the matrix, as given by Eq. 3.

Figures 3, 4, 5, and 6 show the graphical results for each observable, plotted over a temperature range that captures the broad three temperature regimes of interest. For each, the critical temperature  $T_C$  is highlighted.

For 4 and 5, in addition to our results the expected behaviour for an infinitely large Ising System is plotted, and residuals are taken. Notably, this is not a curve fit, and the expected value of these parameters for a given temperature  $T$  are calculated exactly from theory without any free parameters.

Lastly, to pictorially see how the “thermodynamic decision-making” process of the Metropolis Hastings algorithm functions, we plot the acceptance probability as a function of the change in energy,  $\delta E$  of the LED model that would result in a state flip. The acceptance probability is given explicitly in Eq. 6. The behaviour for each temperature regime is also be plotted.

### Energy as a Function of Temperature

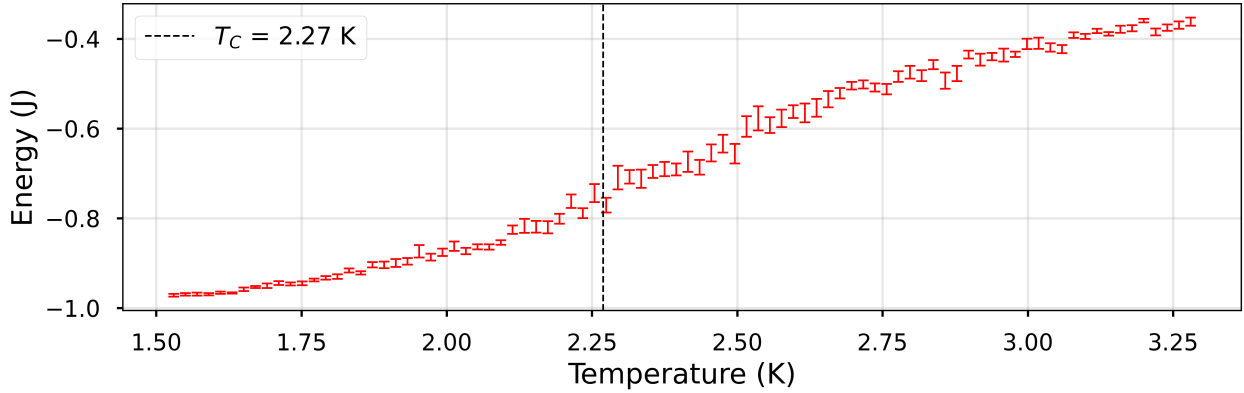


Figure 3: Energy of the LED Ising system for a temperature range spanning all regimes.

### Magnetisation as a Function of Temperature

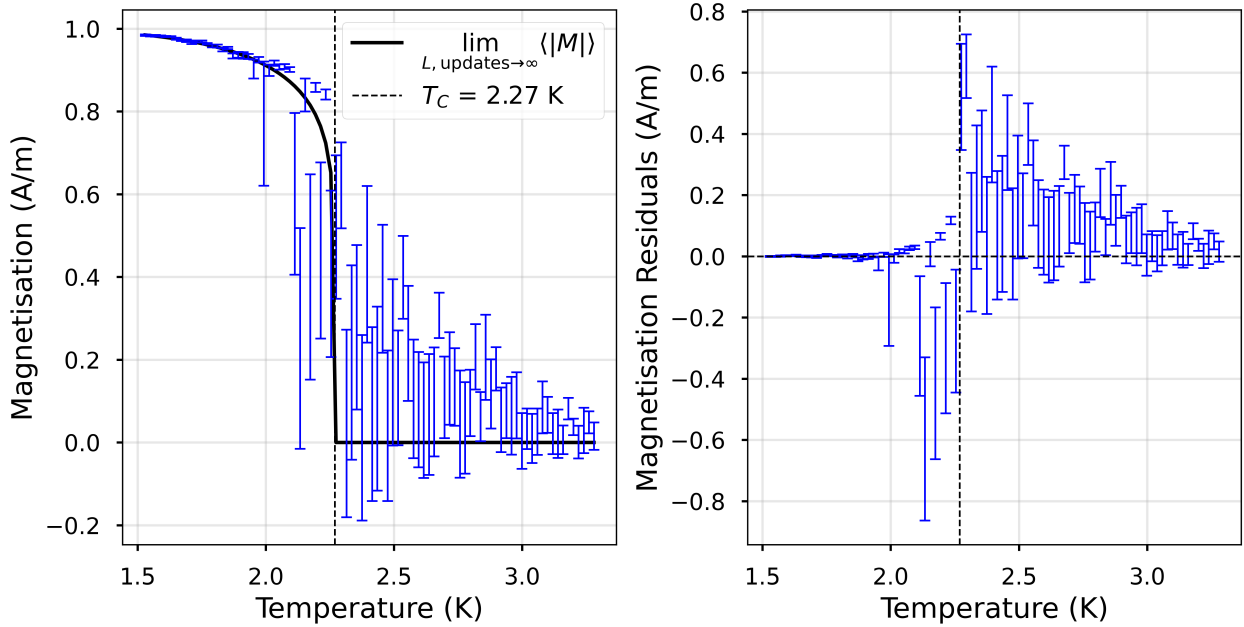


Figure 4: Magnetisation of the LED Ising system, for a temperature spanning all regimes. Also plotted: expected magnetisation in the limit of a large Ising system, in the limit of many update rounds, and residuals of measured magnetisation against this expectation. The  $\chi^2$  of measured  $|M|$  against  $\lim_{L,\text{updates}\rightarrow\infty}\langle|M|\rangle$  is  $4.128 \times 10^3$ , which is expected with probability  $p \approx 0.00$ .

## Specific Heat as a Function of Temperature with Residuals

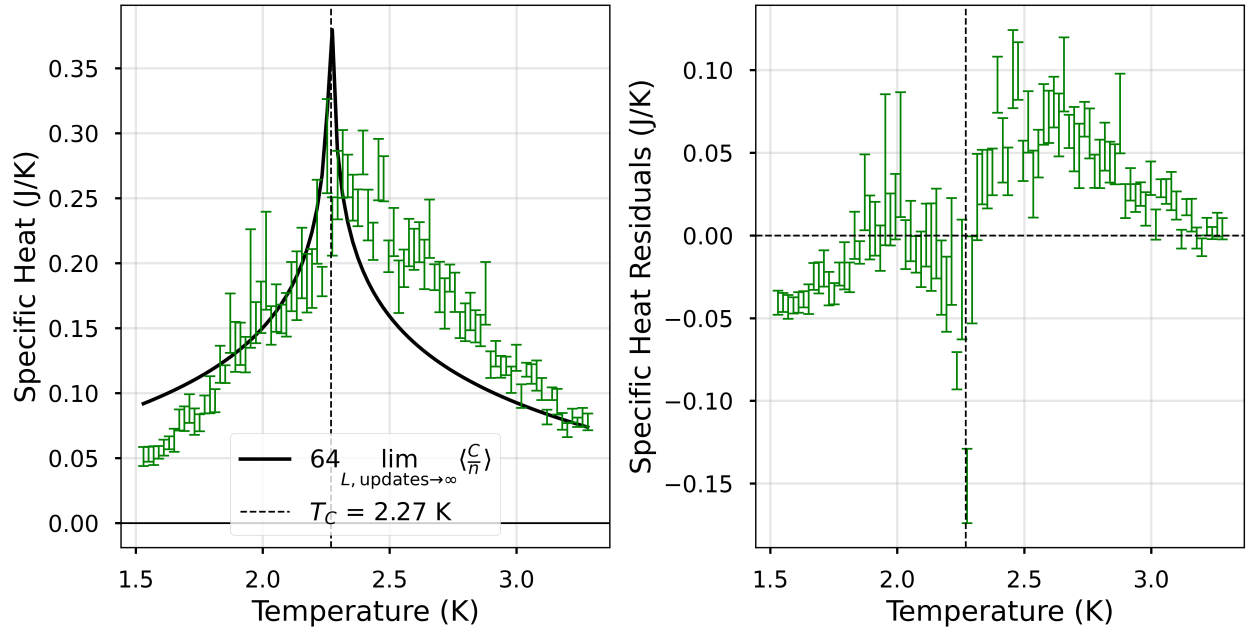


Figure 5: Specific Heat of the LED Ising system, for temperature spanning all regimes. Also plotted: expected specific heat per atom, multiplied by 64 (*the number of atoms in our system*), in the limit of a large Ising system and of many update rounds. On the right: residuals of our measured  $C$  against this expectation. The  $\chi^2$  of  $C$  against  $64 \lim_{n, \text{updates} \rightarrow \infty} \langle C/n \rangle$  is  $6.132 \times 10^5$ , which is expected with probability  $p \approx 0.00$ .

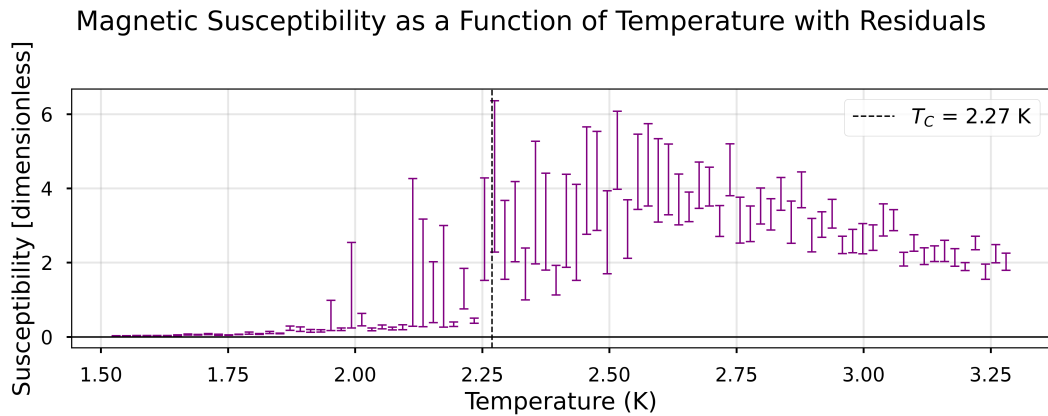


Figure 6: Magnetic susceptibility of the LED Ising system, for a temperature spanning all regimes.

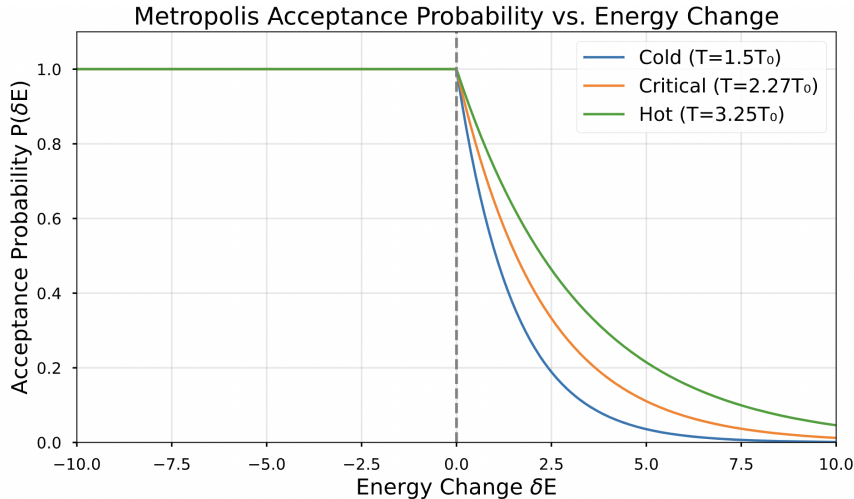


Figure 7: The probability distribution according to the Metropolis Hastings routine for the change in energy  $\delta E$  from the flipping of some dipole spin, for each of the temperature regimes.

## 4 Discussion

Figure 3 displays the expected energy curve: deeply negative for low-temperature states, where almost all the dipoles are aligned, and less negative as temperature increases.

Inspecting the measurements for Magnetisation (Figure 4) and Specific heat (Figure 5), it's visually quite clear that overall behaviour approximates that expected for an infinitely large Ising System. The absurdly improbable  $\chi^2$  values ( $4.128 \times 10^3$  and  $6.132 \times 10^5$ ) emphatically show that the behaviour within this small system follows a far more complex curve [8], and cannot be trivially approximated with large-scale limiting dynamics without losing statistically significant detail.

In Figure 4, scanning from high temperature down towards  $T_C$ , the mean value for magnetisation remains close to zero, while the size of uncertainties vastly increase. This supports the physical intuition from Figure 2: as the system approaches the phase transition, the average size of relatively coherent pockets increases. At the moment of any one observation at  $T = T_C + \epsilon$ , then, the chances of finding the system dominated by Up or Down is high but, between uncorrelated measurements, the choice of which exact state will dominate is

random.

Scanning lower further in temperature, crossing  $T_C$ , the mean value begins to climb upwards. Below  $T_C$ , it's no longer possible to wait long enough to have measurement uncorrelated with each other, and the overall system has frozen into one of two states.

Lower still, and the uncertainty diminishes again, as the size of the largest deviations becomes small - with any small spin-down pockets less likely to be correlated with each other.

Notably, in the region slightly above the critical temperature  $T > T_C$ , measurements that should have an expectation of 0 show some consistent positive bias, likely due to the limited number of updates between measurements. Although 0 is consistently within the window of uncertainty in this region, the measurements are *far too consistent* between subsequent temperature points to be truly uncorrelated (a problem true to a lesser extent below  $T_C$ , too). This suggests our choice for a uniform wait-time between measurements was not large enough to draw a totally random sample.

In Fig. 7, more insight is revealed into why the patterns in Fig. 2 are observed. In the cold regime ( $T = 1.5T_0$ ), the curve shows the steepest exponential decay for  $\delta E > 0$ , indicating the Monte Carlo routine rarely accepts energy-increasing moves. This reflects how low thermal energy suppresses fluctuations, forcing the system to tend toward energy minima (ordered phases). In contrast, the hot regime ( $T = 3.25T_0$ ) exhibits that the acceptance criterion is more lenient for larger  $\delta E > 0$ , hence a wider breath of flipped states will occur, and will approach the limit that each LED cell has a uniform and independent probability of being turned on or off. This is exhibited in the “salt-and-pepper” pattern in Fig. 2.

## 5 Conclusion

This experiment successfully demonstrated the qualitative behaviour of the 2D Ising Model using an  $8 \times 8$  LED matrix as a physical analogue for a magnetic domain. Leveraging a Monte Carlo simulation and sweeping through a range of effective simulated temperature environments, the hot, cold, and critical temperature regimes can be both observed in real-

time and quantitatively examined through various thermodynamic observables. As predicted by theoretical hypothesis, the cold regime resulted in a homogenously oriented spin domain; thereby maximizing the net magnetization of the system. However, by virtue of the acceptance criterion in the Monte Carlo simulation, the cold regime curtails large changes in energy and hence tends towards an energy minimum in this regime. On the other hand, in the hot regime, where the energy of the system configuration is maximal, each LED state becomes equally likely, hence it is expected on expectation that roughly half of the LED matrix is lit up, resulting again, in expectation, in a negligible magnetisation magnitude. It is at the Curie temperature where this transition precisely happens - that is, the smallest value of temperature for which the system spontaneously aligns such that the magnetization vanishes. Below this temperature, the characteristic ferromagnetic properties are observed. For future exploration, it may be substantive to explore different orthodox models to simulate a 2D Ising Model, such as Glauber's algorithm. By contrast to Metropolis Hastings, Glauber's acceptance criterion is based on the Fermi function, and its change in energy is due to a summation of the spins that are orthogonally adjacent neighbours.

## References

- [1] C. Kuelske, “The ising model: Highlights and perspectives,” 2025. [Online]. Available: <https://arxiv.org/abs/2501.05394> 1
- [2] D. V. Schroeder, *Chapter 8*. Oxford Press, 1999, p. 339–353. [Online]. Available: <https://archive.org/details/an-introduction-to-thermal-physics-daniel-schroeder> 1
- [3] P. Alimohamadi and G. J. Ferland, “A practical guide to the partition function of atoms and ions,” *Publications of the Astronomical Society of the Pacific*, vol. 134, no. 1037, p. 073001, Jul. 2022. [Online]. Available: <http://dx.doi.org/10.1088/1538-3873/ac7664> 1
- [4] X. Lu, R. Fei, and L. Yang, “Curie temperature of emerging two-dimensional magnetic structures,” *Physical Review B*, vol. 100, no. 20, Nov. 2019. [Online]. Available: <http://dx.doi.org/10.1103/PhysRevB.100.205409> 2

- [5] L. Onsager, “Crystal statistics. i. a two-dimensional model with an order-disorder transition,” *Phys. Rev.*, vol. 65, pp. 117–149, Feb 1944. [Online]. Available: <https://link.aps.org/doi/10.1103/PhysRev.65.117>
- [6] R. P. Dobrow. Boston, MA: Wiley, 2016, p. 181–212.
- [7] X. Wu, R. Zheng, N. Izmailian, and W. Guo, “Accurate expansions of internal energy and specific heat of critical two-dimensional ising model with free boundaries,” *Journal of Statistical Physics*, vol. 155, no. 1, p. 106–150, Feb. 2014. [Online]. Available: <http://dx.doi.org/10.1007/s10955-014-0942-x>
- [8] T. Takimi, “Prescription for choosing an interpolating function,” *Journal of Mathematical Physics*, vol. 57, no. 2, Jan. 2016. [Online]. Available: <http://dx.doi.org/10.1063/1.4939710>